Intramembranous processing by γ-secretase regulates reverse signaling of ephrin-B2 in migration of microglia

Running title (45 characters): **γ-secretase/ephrinB2 and microglial migration**

Nadja Kemmerling[1], Patrick Wunderlich[1], Sandra Theil[1], Bettina Linnarzt-Gerlach[4], Nils Hersch[2], Bernd Hoffmann[2], Bart de Strooper[3], Harald Neumann[4], Jochen Walter[1]*

[1] Department of Neurology, University of Bonn, 53127 Bonn, Germany

[2] Institute of Complex Systems, ICS-7 Biomechanics, Forschungszentrum Jülich GmbH, 52425 Jülich, Germany

[3] KULeuven and Flanders Interuniversitary Institute for Biotechnology (VIB), Centre for Human Genetics, 3000 Leuven, Belgium

[4] Institute of Reconstructive Neurobiology, University of Bonn, 53127 Bonn, Germany

Word count:

Abstract:	158
Introduction:	556
Materials and Methods:	1392
Results:	1781
Discussion:	1432
Acknowledgements:	47
References:	1524
Figure legends:	1775
Total:	8665

*__correspondence__:
Jochen Walter,
Address: Sigmund-Freud-Str. 25,
53127 Bonn.
Phone: 0049 228 287 19782.
E-mail: jochen.walter@ukb.uni-bonn.de

Main points: γ-Secretase cleaves ephrin-B2 in microglia. The resultant ephrin-B2 intracellular domain regulates phosphorylation of Src/FAK, podosomal dynamics, and microglial motility. γ-Secretase regulates reverse signalling of ephrin-B2 in microglia..

TOCI:

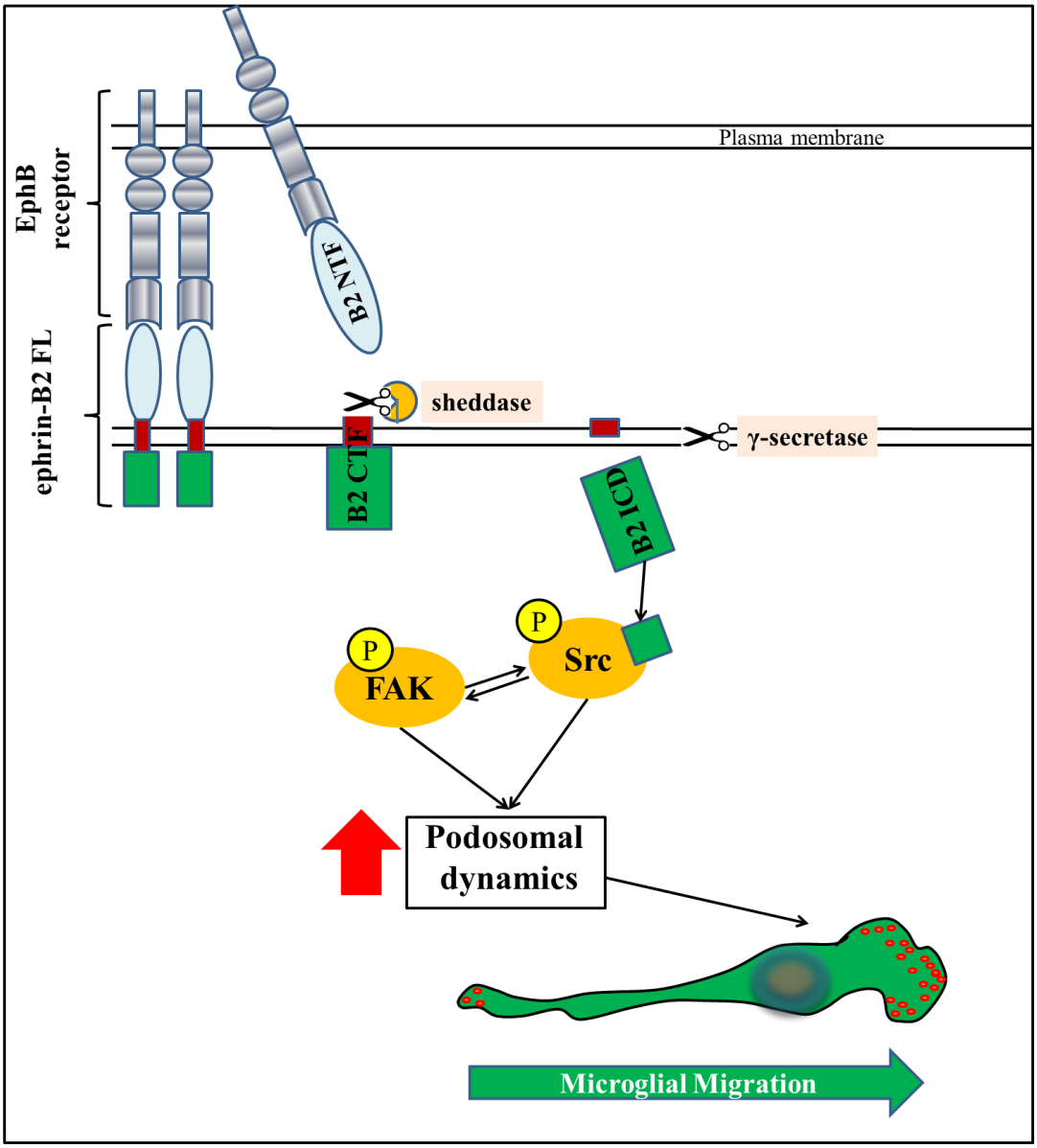

Key words: Ephrin-B, γ-secretase, presenilin, Src, FAK, microglia, podosomes, migration

Abstract

The Eph-ephrin system plays pivotal roles in cell adhesion and migration. The receptor-like functions of the ephrin ligands allow the regulation of intracellular processes via reverse signaling. γ-Secretase mediated processing of ephrin-B has previously been linked to activation of Src, a kinase crucial for focal adhesion and podosome phosphorylation. Here, we analyzed the role of γ-secretase in the stimulation of reverse ephrin-B2 signaling in the migration of embryonic stem cell derived microglia (ESdM). The proteolytic generation of the ephrin-B2 intracellular domain (ICD) by γ-secretase stimulates Src and focal adhesion kinase (FAK). Inhibition of γ-secretase decreased the phosphorylation of Src and FAK, and reduced cell motility. These effects were associated with enlargement of the podosomal surface. Interestingly, expression of ephrin-B2 ICD could rescue these effects, indicating that this proteolytic fragment mediates the activation of Src and FAK, and thereby regulates podosomal dynamics in microglial cells. Together, these results identify γ-secretase as well as ephrin-B2 as regulators of microglial migration.

Introduction

Eph receptors constitute a large family of receptor tyrosine kinases that are regulated by ephrin ligands, hereafter referred to as ephrins. The Eph-ephrin system plays fundamental roles in embryogenesis, development and adulthood by orchestrating cell interaction and migration, differentiation and cell survival (Klein and Kania 2014; Pasquale 2008). It is capable of bidirectional signaling, in which not only the receptors, but also the ephrins regulate multiple intracellular signaling pathways. The signaling via Eph receptors and ephrins is termed 'forward' and 'reverse' signaling, respectively (Holland et al. 1996). The ephrins comprise two groups. While ephrin-A family members are attached to the membrane by a glycosylphosphatidylinositol (GPI) anchor, ephrin-B family members are type I transmembrane proteins with several signaling domains in their cytoplasmic tail. It has been shown that several Eph receptors as well as ephrin-Bs can undergo proteolytic processing by ectodomain shedding and intramembranous cleavage (Atapattu et al. 2014; Georgakopoulos et al. 2006; Pascall and Brown 2004; Tomita et al. 2006). Ectodomain shedding involves proteases of the A disintegrin and metalloproteinase (ADAM) (Janes et al. 2005) or matrix-metalloprotease (MMP) families (Tanaka et al. 2007). The resultant membrane-bound C-terminal fragments (CTFs) can then undergo intramembranous processing by γ-secretase (De Strooper and Annaert 2010; Langosch et al. 2015). This type of regulated intramembranous proteolysis (RIP) has previously been demonstrated for ephrin-B2 (Georgakopoulos et al. 2006), and later also for EphB2 (Litterst et al. 2007; Xu et al. 2009) and EphA4 (Inoue et al. 2009). The γ-secretase mediated cleavage of ephrin-B2 upon EphB2 receptor binding regulates activity of Src in murine embryonic fibroblasts (MEF) (Georgakopoulos et al. 2011; Waschbusch et al. 2009).

Src and the focal adhesion kinase (FAK/PTK2) are important kinases which regulate protein phosphorylation involved in the assembly and disassembly of focal adhesion sites (FAS) and podosomes (Frame 2004; Mitra et al. 2005; Schlaepfer and Mitra 2004). Ephrin-Bs are able to recruit proteins via their four Src homology (SH) 2 binding domains and their PDZ binding domain. Besides Src, ephrin-Bs also attract proteins like growth factor receptor bound protein 4 (Grb4) (Cowan and Henkemeyer 2001; Segura et al. 2007), which is involved in focal adhesion disassembly, and PDZ-domain binding regulator of heterotrimeric G protein signaling (PDZ-RGS) (Lu et al. 2001), which has been shown to link ephrin-B reverse signaling to directed migration. Depending on the cell type, cell migration and adhesion is either mediated by FAS or by podosomes, which are large protein complexes localizing to

sites of cell-matrix interactions. Despite similar protein composition, podosomes are structurally different from FAS (Linder and Aepfelbacher 2003). They are mostly expressed by phagocytic cells with high motility.

The formation of podosomes is also essential for migration of microglia (Vincent et al. 2012). Microglial migration and motility enables these cells to reach distinct locations during development, and in physiological and pathophysiological conditions of the adult brain. Microglia exert a variety of functions in the brain and are associated with different neurological diseases, such as multiple sclerosis, Alzheimer's disease, Parkinson's disease, and ischemic brain diseases (Fu et al. 2014; Prinz and Priller 2014). Here, we demonstrate that stimulation of reverse ephrin-B2 signaling in embryonic stem cell derived microglia (ESdM) involves γ-secretase dependent generation of an ephrin-B2 intracellular domain (ICD). This proteolytic cleavage product stimulates the phosphorylation and activity of both c-Src and FAK. Inhibition of γ-secretase impairs reverse ephrin-B2 signaling and results in decreased podosome dynamics and migration of microglia.

Materials and Methods

Cell culture

Hek293FT cells and murine primary microglia were maintained in Dulbecco´s Modified Eagle´s Medium (DMEM) GlutamaxTM containing 4.5 g/l D-glucose supplemented with 10 % fetal calf serum (FCS, PAN) and 1 % Penicillin/Streptomycin solution (50 U/ml Penicillin, 50 µg/ml Streptomycin). Murine WT and PSdKO embryonic stem cells were generated as described before (Herreman et al. 1999). ES cells from wild type (WT) and presenilin-1/2 double knockout (PSdKO) mice were differentiated into microglia (ESdM) as reported previously (Beutner et al. 2010) and were maintained in DMEM F-12 containing 1×N2 supplement, 0.48 mM L-glutamine, 5.3 µg/ml−1 D-glucose, HEPES and 1 % penicillin/streptomycin solution (50 U/ml penicillin, 50 µg/ml streptomycin) at 37°C, 95 % humidity and 5 % CO_2 (Beutner et al. 2010). The ESdM were extensively characterized previously and closely resemble primary microglia under normal and stimulated conditions (Aslanidis et al. 2015; Beins et al. 2016; Beutner et al. 2013) FACS and semi-quantitative RT-PCR also that ESdM derived from PSdKO cells and transfected with PS1 WT or the inactive PS1 showed similar expression pattern of several surface marker proteins and mRNAs of myeloid cells(supplementary information, supplementary figure 1).

cDNA constructs, virus production and cell transduction

For constitutive overexpression, the Lenti-X Tet-On Advanced System (Clontech, Mountain View, CA) was modified by replacing the cytomegalovirus promoter of the pLVX-Tet-On plasmid with the elongation factor 1 (EF1) α promoter, resulting in the pLVX-EF1α vector. The pLVX-EF1α vector was a generous gift from Dr. Jerome Mertens (University of Bonn). Human ephrin-B2 full-length (NM_004093.3) or fragments closely resembling the C-terminal fragment (CTF) or intracellular domain (ICD) were amplified by PCR. PCR products were restricted with MluI and BamHI and ligated into the pLVX-EF1α vector. Production of lentiviral particles was performed as previously described (Kutner et al. 2009). Briefly, HEK-293FT cells were co-transfected with the packaging plasmid psPAX2, the envelope plasmid pMD2.G, and the respective lentiviral vector plasmid. Viral particles were enriched by incubation with polyethyleneglycol 6000 and consecutive centrifugation. Presenilin expressing and WT ESdM were transduced with the different ephrin-B2 constructs overnight. After antibiotic selection, cells were cultured in the presence of 2 µg/mL puromycin (Sigma-Aldrich).

Primary antibodies

For immunocytochemistry and Western immunoblot analysis the following antibodies were used: C-terminal ephrin-B Ab316 (SAB4300455, Sigma-Aldrich); N-terminal ephrin-B2: (sc-15397, Santa Cruz), N-terminal ephrin-B2 (used in Fig.1 only; MABC127, Millipore); actin (A1978, Sigma-Aldrich); Cell Fractionation Antibody Sampler Kit, containing MEK1/2, AIF, Histone H3 and Vimentin (11843, Cell Signaling Technology); pSrc (Y418) (44660G, Life Technologies); Src (05-184, Millipore); pFAK (Y397) (3283S, Cell signaling technology); Presenilin (C-loop, rb3109, Eurogentec (Prager et al. 2007)); Phosphotyrosine (05-321, Millipore).

Precipitation of proteins with trichloroacetic acid (TCA)

Cell culture supernatants were collected and cleared from cellular debris by centrifugation for 5 min at 300xg. Sodium desoxycholic acid was added to a final concentration of 0.02 % and incubated for 15 min. TCA was then added to a final concentration of 10 %. Next, mixtures were incubated for 1 h at room temperature. Precipitated proteins were collected by centrifugation for 15 min at 16,000xg at 4°C and washed twice with ice-cold acetone. The washed pellets were air-dried, resuspended in 10 µl of Tris-SDS buffer (50 mM Tris, 1 %

SDS in dH2O), and incubated for 10 min at 50°C. Finally, 2x LDS-sample buffer was added, and samples were subjected to separation by NuPAGE (Life Technologies). Image acquisition: ECL imager, Quantity One Software (Biorad). Densitometric analysis of Western blots: ImageJ software.

Cell lysis and cell fractionation

All centrifugation steps were done at 4°C, all other steps were done on ice. For whole cell lysis, cells were incubated 15 min with STEN lysis buffer (50 mM Tris, 150 mM NaCl, 2 mM EDTA, 1 % Nonidet P-40, 1 % Triton X-100, dithiothreitol (DTT), pH 7.4). Homogenates were cleared by centrifugation for 15 min at 16000xg. For cell fractionation, cells were incubated in hypotonic buffer (10 mM Tris, 0.1 mM EGTA, 25 mM β-glycerophosphate, 1 mM dH2O, pH 7.6) for 15 min, followed by passing the suspension through a needle. Cell nuclei were pelleted by centrifugation (10 min at 300xg and 4°C) and were then incubated in buffer C (25 % glycerol, 20 mM HEPES, 0.4 M NaCl, 1 mM EDTA (pH 8.0), 1 mM EGTA, 25 mM β-glycerophosphate, 1 mM DTT) for 15 min. The supernatant containing cytosolic and membrane fraction was centrifuged at 16000xg for 1 h. After centrifugation, the pellet containing the membrane was incubated with STEN lysis buffer as previously described. All buffers contained protease inhibitor (Complete, Roche) and phosphatase inhibitor (PhosSTOP, Roche). Membrane and nuclear fractions were again centrifuged for 15 min at 16000xg. Nuclear, cytosolic and membrane supernatants were mixed with LDS loading dye (containing 100 mM DTT), boiled for 10 min at 70°C and used for NuPAGE protein separation (Life Technologies). For immunoblotting, proteins were transferred to a nitrocellulose membrane that was then probed with the indicated antibodies. Bound antibodies were detected using HRP-conjugated secondary antibodies (Pierce) and subsequent treatment with Amersham ECL Select (GE Healthcare). Image acquisition: ECL imager, Quantity One Software (Biorad). Densitometric analysis of Western blots: ImageJ software.

In-Cell Western

Cells were seeded at 80 % confluence and cultured overnight in a 96 well dish (Vision Plate 96, black, 4titude) under previously described conditions. Subsequently, cells were fixed with 4 % paraformaldehyde (PFA) in TRIS buffered saline (TBS), permeabilized (TBS supplemented with 0.25 % Triton X-100) and incubated with blocking solution (Licor blocking solution:TBS, 1:1) for 1 h at RT. Then, cells were incubated with primary

antibodies in 5x diluted blocking solution for 1 h at RT (pSrc/Src or pFAK/FAK). Following antibody incubation, cells were washed and incubated with mouse IRDye 680RD (Licor) and with rabbit IRDye 800CW (Licor) for 1 h at RT. For detection, TBS without additives was added to the wells. Images were taken (quality: high, resolution: 169 µm, focus: 4 mm) with the Licor Odyssey CLx and brightness of wells was measured using the Image studio software for Odyssey. Further protocols are available at http://biosupport.licor.com/docs/TechNote_SubclassSpecAb.pdf.

Immunocytochemistry and microscopy

For immunocytochemistry primary microglia (5000/cm^2) were seeded onto glass coverslips. After 48 h, cells were washed with serum free medium, 50 % of medium was removed and replaced by 4 % PFA in TBS. Subsequently, cells were quenched with 50 mM NH_4Cl in TBS and permeabilized with a 0.25 % Triton X-100 solution in TBS. Unspecific binding was blocked by using 5 % BSA in TBS containing 0.125 % Triton X-100. After primary antibody incubation, cells were washed three times with washing buffer (0.125 % Triton X-100 in TBS), then secondary antibody (Alexa Fluor 488), 4′,6-Diamidin-2-phenylindol (DAPI) and phalloidin were added. After primary antibody incubation, cells were washed three times with washing buffer (0.125 % Triton X-100 in TBS), were mounted and imaged after 20 h with an AxioVert 200 fluorescence microscope with ZEN analysis Software.

ESdM cells (5000/cm^2) were seeded onto µ-dishes standard bottom (Ibidi, ibiTreat). After 24 h cultivation, 50 % of medium was removed and replaced by 4 % PFA in TBS. Subsequently, cells were quenched, permeabilized and blocked like previously described. Blocking solution contained additional PhosSTOP (Roche) however. After primary antibody incubation, cells were washed three times with washing buffer (0.125 % Triton X-100 in TBS), secondary antibody (Alexa Fluor 488) and phalloidin were added. After three more washing steps, cells were imaged in dishes containing TBS. TIRF was performed on an Nikon Eclipse Ti fluorescence microscope with a x 100 apochromat objective and an EM-CCD camera iXon DU879 (Andor, Oxford). Software: NIS-elements. To analyze staining intensity, the leading edge of ESdM was manually delineated, mean brightness (mean brightness/area) of ROI was measured with ImageJ and background was subtracted. In two independent experiments, brightness of at least 20 cells per group/experiment was measured.

Migration Assays

For migration assays, 15 ng/mL CX3CL1 fractalkine (R&D Systems) (according to (Napoli et al. 2009)) containing serum free medium was pipetted into the two filling reservoirs of the µ-slide chemotaxis 3D channel (Ibidi). $3x10^6$ ESdM cells were seeded into the channel. The µ-slide was kept at 37°C and cells were imaged for 8 h (1 frame/5 min). Image sequences were manually analyzed (Manual Tracking plug in, ImageJ) and tracks were subsequently plotted (Chemotaxis and Migration tool, Ibidi). The accumulated distance of the ~10 fastest migrating cells in each group per day was statistically analyzed.

Statistical analysis

For statistical analysis either Student's t-test (unpaired, two-sided), One-Way ANOVA (with Tukey's post hoc test) or Two-Way ANOVA (with Sidak's post hoc test) were used. Confidence level: 95 %. All graphs display mean of data ±SD.

Results

EphB1 receptor binding induces sequential proteolytic processing of ephrin-B2 in microglia

To analyze expression and cleavage of ephrin-B2 proteins in microglia, we first used primary microglia isolated from mouse brain. Immunocytochemical detection with an antibody recognizing the ectodomain of ephrin-B2 revealed expression of endogenous ephrin-B2 in intracellular membranous compartments (Fig. 1A). A protein of ~ 55 kDa, consistent with the expected molecular mass of ephrin-B, was detected by Western immunoblotting (Fig. 1B). In addition, two smaller proteins of ~20 kDa and ~10 kDa were also faintly detected with an antibody directed against the cytoplasmic C-terminal domain of ephrin-B (1-3), indicative for proteolytic processing products (Fig. 1B). Especially the smaller processing products could only be weakly detected in primary microglia. Thus, we also sought to detect ephrin-B in embryonic stem cell derived microglia (ESdM) that closely resemble characteristics of primary microglia (Aslanidis et al. 2015; Beins et al. 2016; Beutner et al. 2013). ESdM can be genetically modified and cultured in larger scale allowing quantitative biochemical and cell biological experiments. Western immunoblotting revealed endogenous expression of ephrin-B. As observed with primary microglia, proteins of ~50 kDa, ~20 kDa, and ~10 kDa were also detected in ESdM (Fig. 1C). These data are consistent with previous results that indicated proteolytic processing of full-length (~50 kDa) ephrin-B2 into a membrane-bound C-terminal fragment (CTF; ~20 kDa), and a soluble intracellular domain (ICD, ~10 kDa) in

fibroblasts and Hek293 cells (Georgakopoulos et al. 2006; Tomita et al. 2006). Overexpression of ephrin-B2 in ESdM resulted in robust detection of the full-length (~50 kDa) protein (Fig. 1D). The signals for the putative CTF (~20 kDa) and ICD (~14 kDa) increased only slightly upon overexpression of ephrin-B2. The ICD resulting from overexpression of ephrin-B2 FL in these cells was ~4 kDa larger than the endogenous fragment since it containes a C-terminal myc tag. Cell treatment with the proteasome inhibitor MG132 had little if any effect on the level of both fragments. The ICD was hardly detectable after inhibtion of the γ-secretase complex by DAPT (Fig. 1C, D), indicating that ICD generation involves γ-secretase activity. Since γ-secretase cleavage requires precedent shedding of globular ectodomains of its protein substrates, we next assessed the release of the ephrin-B2 ectodomain. In conditioned media, a ~30 kDa fragment corresponding to the secreted ectodomain (N-terminal fragment, NTF) of ephrin-B2 was detected (Fig. 2A), indeed suggesting constitutive processing of ephrin-B2 which results in secretion of the NTF and generation of a membrane-tethered CTF in microglia. Interestingly, incubation with a soluble variant of EphB1 significantly increased the shedding of ephrin-B2 in conditioned media (Fig. 2A, B), suggesting regulated proteolytic processing of ephrin-B2 upon interaction with EphB1.

As observed before, the ICD was hardly dectable in cells with endogenous expression of ephrin-B2. However, treatment of ephrin-B2 overexpressing cells with EphB1 significantly increased not only the secretion of the ephrin-B2 NTFs into conditioned media, but also the levels of cellular CTF and ICD (Fig. 2C, D, F, G). These data indicate that interaction with its receptor induces sequential proteolytic processing of ephrin-B2 by ectodomain shedding and subsequent intramembranous cleavage of the resulting CTF. Pharmacological inhibition of γ-secretase with DAPT led to accumulation of CTF and decreased production of the ephrin-B2 ICD (Fig. 2H-J). To confirm the effects of γ-secretase inhibition in a genetic cellular model, we differentiated embryonic stem (ES) cells from presenilin 1/2 double knock out (PSdKO) mice into microglia and transduced them with full-length ephrin-B2 containing lentivirus. In PSdKO ESdM, generation of the ephrin-B2 ICD was completely abolished, while the CTF was significantly increased (Fig. 2H-J). These data demonstrate that the cleavage of the ephrin-B2 CTF and the proteolytic generation of ICD could be fully attributed to intramembranous cleavage by γ-secretase.

Next, we generated ESdM expressing either the ephrin-B2 CTF or the ICD (Fig. 3A, B). Subcellular fractionation revealed exclusive association of full-length ephrin-B2 and its CTF with cellular membranes. Interestingly, the ICD was detected in the cytosolic as well as in the

nuclear fraction (Fig 3C, D). Cell treatment with the proteasome inhibitor MG132 strongly increased ICD levels, indicating efficient degradation of the ICD by the proteasome. This experiment shows that γ-secretase dependent ephrin-B2 cleavage allows liberation of the ephrin-B2 ICD from cellular membranes and its subsequent translocation into the nucleus.

Activation of ephrin-B by EphB1 receptor stimulates phosphorylation of Src and FAK in a γ-secretase dependent manner

To assess the effect of EphB1 receptor induced proteolytic processing on intracellular signaling, ephrin-B2 FL overexpressing cells were stimulated with the soluble ectodomain of the EphB1 receptor. Then, phosphorylation of Src, a critical kinase in ephrin-B signaling was detected using phosphorylation-state specific antibodies. Upon EphB1 exposure a rapid and transient increase in Src phosphorylation within 5 min was induced as shown by both Western immunoblotting (Fig. 4A, B) and In-Cell Western staining (Fig. 4C). Interestingly, inhibition of γ-secretase with DAPT attenuated the stimulated phosphorylation of Src (Fig. 4D, E), indicating that EphB1 induced Src phosphorylation is dependent on γ-secretase activity. Very similar results were also obtained with In-Cell Western analysis of primary microglia (Fig. 4F, G). Cell treatment with the soluble EphB1 receptor also led to strong phosphorylation of FAK (Fig. 4H), a main kinase in the regulation of focal adhesion site dynamics and cell migration. Similar to Src, the stimulation of FAK phosphorylation by EphB1 also peaked at 5 min, suggesting simultaneous activation of both kinases upon EphB1 treatment. The phosphorylation of FAK rapidly decreased reaching basal levels within 5-10 min. after maximum stimulation (Fig. 4H). Inhibition of γ-secretase with DAPT attenuated the EphB1-induced phosphorylation of FAK (Fig. 4I, J). These analyses identify functional γ-secretase as an important component in the EphB1 induced signaling to Src and FAK.

Phosphorylation of Src and FAK is critically invovled in the regulation of cell adesion. To test the involvement of ephrin-B processing in adhesion of microglia, we first analyzed the effect of ephrin-B ligation with EphB1 in the absence or presence of the γ-secretase inhibitor DAPT on adhesion sites in the leading edge (Fig. 5A). TIRF microscopy revealed highly polarized distribution of adhesion sites reminiscent of podosomes containing an F-actin core surrounded by a ring structure consisting of highly tyrosine-phosphorylated scaffold proteins (Linder and Kopp 2005). Cell incubation with EphB1 significantly increased signals for pTyr and actin in podosomes to a very similar extent (Fig. 5 B-E). The surface of the leading edge did not significantly change (Fig. 5F). Surprisingly, in presence of DAPT pTyr and actin

brightness was also significantly increased in comparison to DMSO control treated cells under these conditions (Fig. 5B-E; see below and Fig. 6 and 7).

To further link γ-secretase dependent ephrin-B processing and the activity of Src and FAK, we sought to establish a genetic cellular model expressing functional or inactive presenilin 1 (PS-1). We used ESdM from PS1/2 double knock-out mice (PSdKO) that completely lack γ-secretase activity to re-express either functional wild-type PS1 or a catalytically inactive variant (PS1 D385N, hereafter referred to as PS1 DN). Cells expressing PS1 WT revealed characteristic PS1 CTFs demonstrating efficient endoproteolytic cleavage by presenilinase (Fig. 6A). In contrast, the PS1 DN variant accumulated as a full-length protein. Only minor amounts of PS1 CTFs were detected demonstrating strongly reduced endoproteolytic processing and thus impaired γ-secretase activity.

Interestingly, under unstimulated conditions in the absence of EphB1, ESdM expressing inactive PS1 (PS1 DN) had significantly increased pTyr and actin signals compared to cells expressing functional PS1 (PS1 WT; Fig. 6B, C). Moreover, PS1 WT overexpressing cells responded to EphB1 with increased levels of pTyr and actin in podosomes to similar extent and thus, the ratio of pTyr/actin was not changed (Fig. 6B-D). The average surface of the leading edge was also not significantly affected by the different PS genotypes or stimulation with EphB1 (Fig. 6E). In contrast, ESdM expressing inactive PS1 did not respond to stimulation with EphB1 with a further increase in pTyr and actin signals in podosomes (Fig. 6B, C). In the presence of DAPT, pTyr and actin brightness was also significantly increased in comparison to DMSO control treated cells under these conditions. The data indicate a critical involvement of γ-secretase in the regulation of podosomes by EphB1- ephrin-B signaling.

This was further supported by the finding that microglia which express inactive PS1 DN showed significantly decreased levels of phosphorylated Src and FAK under basal conditions (without stimulation by EphB1) as compared to cells expressing the functional PS1 WT (Fig. 7A–D). Interestingly, re-expression of the ephrin-B2 ICD in PS1 DN cells strongly increased pSrc and pFAK (Fig. 7A-D), further supporting a critical role of the ephrin-B2 ICD generated by γ-secretase in the phosphorylation of Src and FAK.

We took advantage of this genetic model to further assess the role of γ-secretase and the ephrin-B2 ICD in cell adhesion and migration. As observed before (Fig. 6), the signals for actin and pTyr per area were significantly elevated in cells expressing PS1 DN as compared to cells with functional PS1 WT (Fig. 8A-C). Interestingly, expression of the soluble ephrin-B2 ICD in PS1 DN microglia normalized both actin and pTyr signals in podosomes. The

increased pTyr signal was proportional to that of the actin signal. Thus, the ratio of pTyr/actin was similar in cells expressing functional or inactive PS1 (Fig. 8D). The average area of leading egdes in PS1 DN expressing cells was slightly larger than in PS1 WT expressing cells. Additional expression of the ephrin-B2 ICD in PS1 DN normalized the size of leading edges comparable to that of PS1 WT cells (Fig. 8E). These findings suggest that ephrin-B2 reverse signaling is a potent modulator of podosomal dynamics.

γ-Secretase and the ephrin-B2 ICD regulate migration of microglia

Next, we wanted to test whether these changes in podosomal cell adhesion functionally affect cell motility. Migration of ESdM was stimulated with the chemokine CX3CL1 and monitored by live cell microscopy. Cells expressing the inactive PS1 DN variant showed significantly decreased motility as compared to cells expressing functional PS1 WT (Fig 9A, B). Consistent with a critical role of the ephrin-B2 ICD in podosome dynamics, expression of the soluble ICD variant fully rescued the migrational deficit of PS1 DN cells (Fig. 9A, B). The motility of PSdKO ESdM re-expressing functional PS1 was similar to that of naïve ESdM expressing endogenous PS1 (Fig. 9C). In absence of CX3CL1, addition of EphB1 had little if any effect on migration of the cells with the different PS genotype (Fig. 9C). However, pharmacological inhibition of γ-secretase significantly decreased the basal motility of both PSdKO ESdM re-expressing functional PS1 or naïve ESdM. In contrast, γ-secretase inhibition did not further decrease the already low motility of PSdKO ESdM re-expressing the catalytically inactive PS1 DN variant (Fig. 9C). Taken together, these results implicate γ-secretase dependent ephrin-B2 reverse signaling in the regulation of podosomal dynamics and microglial migration.

Discussion

The present data establish a functional connection of γ-secretase mediated processing of ephrin-B2 and podosomal turn-over in the migration of microglial cells. Primary mouse microglia and ESdM endogenously express ephrin-B. Western immunoblotting revealed that full-length ephrin-B undergoes ectodomain shedding resulting in the release of a soluble ectodomain and the generation of a membrane bound CTF. This CTF can undergo cleavage by presenilin-dependent γ-secretase activity. A similar processing pathway was demonstrated in a heterologous expression system previously (Georgakopoulos et al. 2006; Tomita et al. 2006). Shedding of ephrin-B has been shown to involve MMPs (Tanaka et al. 2007) and

ADAMs (Janes et al. 2005; Wei et al. 2010) and is increased by interaction of ephrin-B2 with one of its receptors, including EphB1. Pharmacological as well as genetic inhibition of γ-secretase by DAPT or knock out of presenilins, led to strong accumulation of the ephrin-B2 CTF in cellular membranes and decreased the release of soluble ephrin-B2 ICD. This indicates that γ-secretase is responsible for RIP of ephrin-B2 in microglia. Similar ephrin-B2 ICD generation has been reported in transfected Cos-7 cells and fibroblasts (Georgakopoulos et al. 2006; Tomita et al. 2006). The ephrin-B2 ICD is stabilized by proteasomal inhibition, suggesting efficient turn-over of the ICD in untreated cells. Interaction of ephrin-B2 with EphB receptors strongly increased the production of the ICD. Consistent with our previous data with fibroblasts (Waschbusch et al. 2009), we also observed translocation of the ephrin-B2 ICD to the nucleus. For ephrin-B1, Tomita et al. showed that the juxtamembrane region of the ephrin-B1 ICD is essential for nuclear translocation (Tomita et al. 2006). Many ICDs of γ-secretase substrates, like those of Notch (NICD) and CD44 exert gene regulatory functions (Cui et al. 2006; Jarriault et al. 1995).

In our study, we focussed on membrane proximal signaling events of ephrin-B. The stimulation of ephrin-B2 shedding by soluble EphB1 increased Src phosphorylation within 5 min. Src phosphorylation was impaired by cell treatment with the γ-secretase inhibitor DAPT, showing that EphB1 induced Src activation is γ-secretase dependent. Additionally, EphB1 receptor treatment increased the phosphorylation of FAK on Y397. Autophosphorylation of FAK at Y397 creates a binding site for the SH2 domain of Src and other proteins. Upon recruitment to Y397 phosphorylated FAK, Src can further phosphorylate FAK at Y576 and Y577 to promote maximal FAK activity (Hanks et al. 2003; Mitra et al. 2005). Georgakopoulos et al. (Georgakopoulos et al. 2006; Georgakopoulos et al. 2011) previously showed that ephrin-B2 ICD generation causes an increase of Src activity. The ephrin-B2 ICD was furthermore reported to bind to the Src inhibitor complex PAG/Cbp and Csk and to Src itself, leading to autocatalytic Src activation. In our microglial model, the simultaneous activation of Src and FAK upon stimulation of the EphB-ephrin-B system also suggests complex formation of Src and FAK resulting in increased phosphorylation and activation of both kinases. Interestingly, inhibition of γ-secretase suppressed activation of Src and FAK. These data indicate an important role for RIP of ephrin-B2 in membrane proximal signaling to critical components involved in FAS dynamics. For integrin-dependent stimuli that also promote cell motility, one of the first events associated with FAK activation, is the recruitment of Src kinases into a signaling complex with FAK (Schlaepfer and Mitra 2004). Src phosphorylation of FAK, creates binding sites for SH3 domain containing podosomal

proteins, such as p130 Cas. It has also been shown that cells, which express a kinase-deficient Src variant, also display suppressed FAK phosphorylation, indicating that the low pFAK levels in PSdKO PS1 DN cells may be due to decreased Src activity (Timpson et al. 2001). However, activation of FAK could also involve other ephrin-B binding proteins, like previously shown for Grb4 (Cowan and Henkemeyer 2001).

Reverse signaling of ephrin-B proteins has been found to induce cell repulsion, cytoskeletal reorganization and disassembly of FAS in many cell types (Foo et al. 2006; Rudolph et al. 2014; Tanaka et al. 2003). As mentioned above, cell types that rely on high motility, like macrophages, invasive cancer cells and dendritic cells, often form podosomes instead of FAS. Podosomes constitute a polarized pattern in the cells predetermining the direction of migration. They are recruited to the leading edge, which makes it a suitable cellular location to analyze podosomal turn-over. In this study we found that podosomal turn-over depends on γ-secretase activity. Surprisingly, presenilin knock out resulted in a strongly enlarged podosomal surface in the leading edge. This phenotype resembles the previously described phenotype of a Src mutant lacking its catalytic domain (Fincham et al. 2000; Kaplan et al. 1994; Timpson et al. 2001). This Src variant, which only contains the SH2 and SH3 domains (AA 1-251), translocated to and caused enlargement of FAS, which were extensively phosphorylated despite lack of Src kinase activity (Kaplan et al. 1994). These findings suggest that activation of Src promotes the turn-over of FAS by stimulating FAS disassembly rather than FAS assembly. Furthermore, Ilic et al. showed that cells from FAK knock out mice displayed a larger number of FAS (Ilic et al. 1995), indicating a similar function for FAK. Notably, the impaired podosomal turn-over in microglia without γ-secretase activity could be efficiently reverted by re-expression of the soluble cytoplasmic ICD of ephrin-B2 that resembles the product of γ-secretase cleavage. Together with the finding that Src as well as FAK kinase activity was inhibited by non-functional γ-secretase, these data indicate that γ-secretase mediated processing of ephrin-B2 and liberation of its ICD from cellular membranes regulates podosomal turn-over via phosphorylation of Src and FAK kinase.

The functional relevance of these findings was demonstrated by analysis of microglial migration. Cells with inactive γ-secretase showed significantly impaired migration. The present results resemble findings in kinase-deficient Src, as well as FAK knock out cells, in which low Src and FAK activity and enlarged FAS size were associated with reduced motility (Ilic et al. 1995; Kaplan et al. 1994). Consistent with an important role of the γ-secretase dependent cleavage of ephrin-B2, expression of the soluble ICD fully restored microglial migration (for a schematic representation, see fig. 10).

Cell treatment with a soluble EphB1 receptor stimulated the phosphorylation of Src and FAK and was associated with an increase in podosomal surface. Surprisingly, we also found that cell treatment with EphB1 receptor did not increase microglial migration. The reason for this remains unclear. However, stimulation of microglial migration with the receptor may require selective binding to one side of the cell. It was previously found that binding of the receptor to its ligand causes retraction or attraction from or to the cell carrying the complement EphB receptor, in order to direct cells during development (Allen-Sharpley and Cramer 2012; Petros et al. 2010; Smith et al. 1997). Binding of soluble receptor to its ligand at the plasma membrane in a non-polarized manner, may not provide the information required for directed migration and therefore not stimulate migratory activity.

The complete homology of the three human ephrin-B family members of the signaling domain sequence, strongly suggests a similar function in the regulation of microglial migration between family members. Ephrin-Bs are involved in the regulation of neuronal migration during development (Santiago and Erickson 2002; Senturk et al. 2011; Wang and Anderson 1997). Furthermore, impaired migration upon inhibition of γ-secretase has already been observed in other cell types. For example, the γ-secretase inhibitor DAPT or the overexpression of the γ-secretase substrate proteins voltage-gated sodium channel β2-subunit CTF and Nectin CTF inhibited migration of SH-SY5Y cells (Kim et al. 2005). Additionally, the γ-secretase inhibition by GSI34 has been shown to attenuate migration of two breast cancer cell lines (MDA MB231, 4T1) (Villa et al. 2014). We also observed impaired migration of primary mouse microglia upon inhibition of γ-secretase with DAPT or siRNA mediated knockdown of ephrin B2 (data not shown), further supporting a functional role of this system in the regulation microglial migration. Thus, the proteolytic processing of ephrin-B2 by γ-secretase and its role in cell migration is observed in both ESdM and primary microglia. However, it will be important to assess potential quantitative differences between the ESdM model and authentic microglia, and also test the physiological relevance of these findings *in vivo*.

The activation and migration of microglia could play important roles in chronic neuroinflammatory processes associated with several neurodegenerative diseases (Cameron and Landreth 2010; Heneka et al. 2015). Notably, a mutation of EphA4, a receptor that binds to ephrin-As as well as ephrin-Bs, has recently been associated with an increased risk for AD (Hollingworth et al. 2011), suggesting an involvement of the Eph-ephrin system in AD. Cisse et. al furthermore found that overexpression of hippocampal EphB2, which regulates NMDA receptor function, could reverse long term potentiation and memory deficits in amyloid

precursor protein transgenic mice (Cisse et al. 2011). Our data indicate an additional role of this system in the regulation of microglial migration. Thus, it will be interesting to further investigate the potential contribution of Eph-ephrin signaling and γ-secretase in inflammation during neurodegeneration.

Acknowledgements: We are grateful to Dr. C. Beutner for the generation of ESdM, and A. Vieira-Saecker and Dr. M. Heneka for providing primary microglia. This project was supported by the DFG (SFB645, KFO177, and SFB704). H. Neumann is member of the DFG-funded excellence cluster 'ImmunoSensation' (EXC 1023).

References

Allen-Sharpley MR, Cramer KS. 2012. Coordinated Eph-ephrin signaling guides migration and axon targeting in the avian auditory system. Neural Dev 7:29.

Aslanidis A, Karlstetter M, Scholz R, Fauser S, Neumann H, Fried C, Pietsch M, Langmann T. 2015. Activated microglia/macrophage whey acidic protein (AMWAP) inhibits NFkappaB signaling and induces a neuroprotective phenotype in microglia. J Neuroinflammation 12:77.

Atapattu L, Lackmann M, Janes PW. 2014. The role of proteases in regulating Eph/ephrin signaling. Cell Adh Migr 8:294-307.

Beins E, Ulas T, Ternes S, Neumann H, Schultze JL, Zimmer A. 2016. Characterization of inflammatory markers and transcriptome profiles of differentially activated embryonic stem cell-derived microglia. Glia 64:1007-20.

Beutner C, Linnartz-Gerlach B, Schmidt SV, Beyer M, Mallmann MR, Staratschek-Jox A, Schultze JL, Neumann H. 2013. Unique transcriptome signature of mouse microglia. Glia 61:1429-42.

Beutner C, Roy K, Linnartz B, Napoli I, Neumann H. 2010. Generation of microglial cells from mouse embryonic stem cells. Nat Protoc 5:1481-94.

Cameron B, Landreth GE. 2010. Inflammation, microglia, and Alzheimer's disease. Neurobiol Dis 37:503-9.

Cisse M, Halabisky B, Harris J, Devidze N, Dubal DB, Sun B, Orr A, Lotz G, Kim DH, Hamto P and others. 2011. Reversing EphB2 depletion rescues cognitive functions in Alzheimer model. Nature 469:47-52.

Cowan CA, Henkemeyer M. 2001. The SH2/SH3 adaptor Grb4 transduces B-ephrin reverse signals. Nature 413:174-9.

Cui W, Ke JZ, Zhang Q, Ke HZ, Chalouni C, Vignery A. 2006. The intracellular domain of CD44 promotes the fusion of macrophages. Blood 107:796-805.

De Strooper B, Annaert W. 2010. Novel research horizons for presenilins and gamma-secretases in cell biology and disease. Annu Rev Cell Dev Biol 26:235-60.

Fincham VJ, Brunton VG, Frame MC. 2000. The SH3 domain directs acto-myosin-dependent targeting of v-Src to focal adhesions via phosphatidylinositol 3-kinase. Mol Cell Biol 20:6518-36.

Foo SS, Turner CJ, Adams S, Compagni A, Aubyn D, Kogata N, Lindblom P, Shani M, Zicha D, Adams RH. 2006. Ephrin-B2 controls cell motility and adhesion during blood-vessel-wall assembly. Cell 124:161-73.

Frame MC. 2004. Newest findings on the oldest oncogene; how activated src does it. J Cell Sci 117:989-98.

Fu R, Shen Q, Xu P, Luo JJ, Tang Y. 2014. Phagocytosis of microglia in the central nervous system diseases. Mol Neurobiol 49:1422-34.
Georgakopoulos A, Litterst C, Ghersi E, Baki L, Xu C, Serban G, Robakis NK. 2006. Metalloproteinase/Presenilin1 processing of ephrinB regulates EphB-induced Src phosphorylation and signaling. EMBO J 25:1242-52.
Georgakopoulos A, Xu J, Xu C, Mauger G, Barthet G, Robakis NK. 2011. Presenilin1/gamma-secretase promotes the EphB2-induced phosphorylation of ephrinB2 by regulating phosphoprotein associated with glycosphingolipid-enriched microdomains/Csk binding protein. FASEB J 25:3594-604.
Hanks SK, Ryzhova L, Shin NY, Brabek J. 2003. Focal adhesion kinase signaling activities and their implications in the control of cell survival and motility. Front Biosci 8:d982-96.
Heneka MT, Golenbock DT, Latz E. 2015. Innate immunity in Alzheimer's disease. Nat Immunol 16:229-36.
Herreman A, Hartmann D, Annaert W, Saftig P, Craessaerts K, Serneels L, Umans L, Schrijvers V, Checler F, Vanderstichele H and others. 1999. Presenilin 2 deficiency causes a mild pulmonary phenotype and no changes in amyloid precursor protein processing but enhances the embryonic lethal phenotype of presenilin 1 deficiency. Proc Natl Acad Sci U S A 96:11872-7.
Holland SJ, Gale NW, Mbamalu G, Yancopoulos GD, Henkemeyer M, Pawson T. 1996. Bidirectional signalling through the EPH-family receptor Nuk and its transmembrane ligands. Nature 383:722-5.
Hollingworth P, Harold D, Sims R, Gerrish A, Lambert JC, Carrasquillo MM, Abraham R, Hamshere ML, Pahwa JS, Moskvina V and others. 2011. Common variants at ABCA7, MS4A6A/MS4A4E, EPHA1, CD33 and CD2AP are associated with Alzheimer's disease. Nat Genet 43:429-35.
Ilic D, Furuta Y, Kanazawa S, Takeda N, Sobue K, Nakatsuji N, Nomura S, Fujimoto J, Okada M, Yamamoto T. 1995. Reduced cell motility and enhanced focal adhesion contact formation in cells from FAK-deficient mice. Nature 377:539-44.
Inoue E, Deguchi-Tawarada M, Togawa A, Matsui C, Arita K, Katahira-Tayama S, Sato T, Yamauchi E, Oda Y, Takai Y. 2009. Synaptic activity prompts gamma-secretase-mediated cleavage of EphA4 and dendritic spine formation. J Cell Biol 185:551-64.
Janes PW, Saha N, Barton WA, Kolev MV, Wimmer-Kleikamp SH, Nievergall E, Blobel CP, Himanen JP, Lackmann M, Nikolov DB. 2005. Adam meets Eph: an ADAM substrate recognition module acts as a molecular switch for ephrin cleavage in trans. Cell 123:291-304.
Jarriault S, Brou C, Logeat F, Schroeter EH, Kopan R, Israel A. 1995. Signalling downstream of activated mammalian Notch. Nature 377:355-8.
Kaplan KB, Bibbins KB, Swedlow JR, Arnaud M, Morgan DO, Varmus HE. 1994. Association of the amino-terminal half of c-Src with focal adhesions alters their properties and is regulated by phosphorylation of tyrosine 527. EMBO J 13:4745-56.
Kim DY, Ingano LA, Carey BW, Pettingell WH, Kovacs DM. 2005. Presenilin/gamma-secretase-mediated cleavage of the voltage-gated sodium channel beta2-subunit regulates cell adhesion and migration. J Biol Chem 280:23251-61.
Klein R, Kania A. 2014. Ephrin signalling in the developing nervous system. Curr Opin Neurobiol 27:16-24.
Kutner RH, Zhang XY, Reiser J. 2009. Production, concentration and titration of pseudotyped HIV-1-based lentiviral vectors. Nat Protoc 4:495-505.
Langosch D, Scharnagl C, Steiner H, Lemberg MK. 2015. Understanding intramembrane proteolysis: from protein dynamics to reaction kinetics. Trends Biochem Sci.
Linder S, Aepfelbacher M. 2003. Podosomes: adhesion hot-spots of invasive cells. Trends Cell Biol 13:376-85.
Linder S, Kopp P. 2005. Podosomes at a glance. J Cell Sci 118:2079-82.

Litterst C, Georgakopoulos A, Shioi J, Ghersi E, Wisniewski T, Wang R, Ludwig A, Robakis NK. 2007. Ligand binding and calcium influx induce distinct ectodomain/gamma-secretase-processing pathways of EphB2 receptor. J Biol Chem 282:16155-63.

Lu Q, Sun EE, Klein RS, Flanagan JG. 2001. Ephrin-B reverse signaling is mediated by a novel PDZ-RGS protein and selectively inhibits G protein-coupled chemoattraction. Cell 105:69-79.

Mitra SK, Hanson DA, Schlaepfer DD. 2005. Focal adhesion kinase: in command and control of cell motility. Nat Rev Mol Cell Biol 6:56-68.

Napoli I, Kierdorf K, Neumann H. 2009. Microglial precursors derived from mouse embryonic stem cells. Glia 57:1660-71.

Pascall JC, Brown KD. 2004. Intramembrane cleavage of ephrinB3 by the human rhomboid family protease, RHBDL2. Biochem Biophys Res Commun 317:244-52.

Pasquale EB. 2008. Eph-ephrin bidirectional signaling in physiology and disease. Cell 133:38-52.

Petros TJ, Bryson JB, Mason C. 2010. Ephrin-B2 elicits differential growth cone collapse and axon retraction in retinal ganglion cells from distinct retinal regions. Dev Neurobiol 70:781-94.

Prager K, Wang-Eckhardt L, Fluhrer R, Killick R, Barth E, Hampel H, Haass C, Walter J. 2007. A structural switch of presenilin 1 by glycogen synthase kinase 3beta-mediated phosphorylation regulates the interaction with beta-catenin and its nuclear signaling. J Biol Chem 282:14083-93.

Prinz M, Priller J. 2014. Microglia and brain macrophages in the molecular age: from origin to neuropsychiatric disease. Nat Rev Neurosci 15:300-12.

Rudolph J, Gerstmann K, Zimmer G, Steinecke A, Doding A, Bolz J. 2014. A dual role of EphB1/ephrin-B3 reverse signaling on migrating striatal and cortical neurons originating in the preoptic area: should I stay or go away? Front Cell Neurosci 8:185.

Santiago A, Erickson CA. 2002. Ephrin-B ligands play a dual role in the control of neural crest cell migration. Development 129:3621-32.

Schlaepfer DD, Mitra SK. 2004. Multiple connections link FAK to cell motility and invasion. Curr Opin Genet Dev 14:92-101.

Segura I, Essmann CL, Weinges S, Acker-Palmer A. 2007. Grb4 and GIT1 transduce ephrinB reverse signals modulating spine morphogenesis and synapse formation. Nat Neurosci 10:301-10.

Senturk A, Pfennig S, Weiss A, Burk K, Acker-Palmer A. 2011. Ephrin Bs are essential components of the Reelin pathway to regulate neuronal migration. Nature 472:356-60.

Smith A, Robinson V, Patel K, Wilkinson DG. 1997. The EphA4 and EphB1 receptor tyrosine kinases and ephrin-B2 ligand regulate targeted migration of branchial neural crest cells. Curr Biol 7:561-70.

Tanaka M, Kamo T, Ota S, Sugimura H. 2003. Association of Dishevelled with Eph tyrosine kinase receptor and ephrin mediates cell repulsion. EMBO J 22:847-58.

Tanaka M, Sasaki K, Kamata R, Sakai R. 2007. The C-terminus of ephrin-B1 regulates metalloproteinase secretion and invasion of cancer cells. J Cell Sci 120:2179-89.

Timpson P, Jones GE, Frame MC, Brunton VG. 2001. Coordination of cell polarization and migration by the Rho family GTPases requires Src tyrosine kinase activity. Curr Biol 11:1836-46.

Tomita T, Tanaka S, Morohashi Y, Iwatsubo T. 2006. Presenilin-dependent intramembrane cleavage of ephrin-B1. Mol Neurodegener 1:2.

Villa JC, Chiu D, Brandes AH, Escorcia FE, Villa CH, Maguire WF, Hu CJ, de Stanchina E, Simon MC, Sisodia SS and others. 2014. Nontranscriptional role of Hif-1alpha in activation of gamma-secretase and notch signaling in breast cancer. Cell Rep 8:1077-92.

Vincent C, Siddiqui TA, Schlichter LC. 2012. Podosomes in migrating microglia: components and matrix degradation. J Neuroinflammation 9:190.

Wang HU, Anderson DJ. 1997. Eph family transmembrane ligands can mediate repulsive guidance of trunk neural crest migration and motor axon outgrowth. Neuron 18:383-96.

Waschbusch D, Born S, Niediek V, Kirchgessner N, Tamboli IY, Walter J, Merkel R, Hoffmann B. 2009. Presenilin 1 affects focal adhesion site formation and cell force generation via c-Src transcriptional and posttranslational regulation. J Biol Chem 284:10138-49.

Wei S, Xu G, Bridges LC, Williams P, White JM, DeSimone DW. 2010. ADAM13 induces cranial neural crest by cleaving class B Ephrins and regulating Wnt signaling. Dev Cell 19:345-52.

Xu J, Litterst C, Georgakopoulos A, Zaganas I, Robakis NK. 2009. Peptide EphB2/CTF2 generated by the gamma-secretase processing of EphB2 receptor promotes tyrosine phosphorylation and cell surface localization of N-methyl-D-aspartate receptors. J Biol Chem 284:27220-8.

Figure legends

Fig. 1 Endogenous expression of ephrin-B2 is in murine primary and ES cell derived microglia. A) Cells were stained with DAPI for nucleus, Phalloidin for actin fibers and ephrin-B2 with an N-terminal ephrin-B2 Ab (in upper panel). Secondary antibody control (lower panel) shows the specificity of ephrin-B2 detection in murine primary microglia. Scale bar: 20 μm. **B)** Detection of endogenously expressed ephrin-B (1-3) family members in murine primary microglia using a C-terminal ephrin-Ab by Western immunoblotting. Ephrin-B FL (full-length) is well detectable, the ephrin-B fragments (CTF, C-terminal fragment; ICD, intracellular domain) are only weakly detectable at longer exposure of membranes (n=1). **C)** In ESdM, a prominent ephrin-B FL, and weaker ephrin-B fragments (ephrin-B CTF and ICD) were detected. Treatment with MG132 (0.1 μM, 4 h) only weakly increased the detection of the ephrin-B ICD levels. Treatment with DAPT (24h, 10 μM) caused decreased ephrin-B ICD levels as compared to the DMSO control (n=2). **D)** ESdM were lentivirally transduced to overexpress full-length ephrin-B2. Treatment with MG132 (0.1 μM, 4 h) increased ephrin-B ICD levels. Treatment with DAPT (24h, 10 μM) decreased ephrin-B ICD levels compared to the DMSO control. Images for ephrin-B2 CTF and ICD are from longer exposure times of membranes than the image for ephrin-B2 FL. Migration of endogenous ephrin-B2 ICDs and the ICD of overexpressed myc-tagged ephrin B2 are indicated by arrows (n=2).

Fig.2: EphB1 receptor induced sequential proteolytic processing of ephrin-B2. A) ESdM were either treated with a control Fc-protein (Ctrl Fc) or the EphB1 receptor protein (EphB1) for 40 minutes. Shedding of endogenous ephrin-B (NTF, N-terminal fragment) is induced by treatment with EphB1 receptor. **B)** Quantification of A) shows significant increase of ephrin-B NTF levels in cell culture medium (TCA precipitated) upon EphB1 receptor treatment of ESdM (n=3). **C-G)** Effects of soluble EphB1 on the proteolytic processing of overexpressed ephrin-B2 in ESdM. Images for ephrin-B2 CTF and ICD resulted from a longer exposure time than the image for ephrin-B2 FL. Cell treatment with EphB1 receptor increased levels of ephrin-B2 NTF in the cell culture medium (D), and of the ephrin-B2 ICD in cell lysates (G). Cellular levels of full-length ephrin-B2 (E), and CTFs (F) were only slightly affected by cell treatment with EphB1 (n=3). **H-J)** Analysis of WT and PSdKO ESdM cells overexpressing ephrin-B2 FL. Treatment with the γ-secretase inhibitor DAPT (24h, 10 μM) increased ephrin-B2 CTF and decreased ephrin-B2 ICD in WT cells. Cells lacking γ-secretase (PSdKO)

showed strong accumulation of the ephrin-B2 CTF and absence of the ICD. All data are represented as means ± SD (n=4).

Fig.3: Ephrin-B2 ICD translocates to nucleus. A) Schematic of ephrin-B2 shedding upon EphB1 receptor binding and cleavage by γ-secretase. 1) Upon extracellular EphB1 receptor binding to ephrin-B2 it is 2) shedded by ADAM secretases, producing the ephrin-B2 NTF and CTF, whereby the latter is still bound to the membrane. 3) Subsequently, the γ-secretase cleaves the ephrin-B2 CTF in its transmembrane region (TMR) to produce the ephrin-B2 ICD. **B)** Schematic of ephrin-B2 FL, CTF and ICD constructs used for overexpression in ESdM. The ephrin-B2 ICD contains several Src homology 2 (SH2) binding domains and one PDZ binding domain. **C)** Representative blot of cell fractionation control. Membrane (marker: AIF), cytosol (marker: MEK1/2) and the nuclear fraction (marker: vimentin). This blot is representative for the fractionation control of all three samples shown in D). M=membrane, C=cytosol, N=nucleus. **D)** Cell fractionation of ESdM overexpressing the ephrin-B2 FL, CTF or ICD constructs. The ephrin-B2 FL and CTF are localized in the membrane. The ephrin-B2 ICD localizes to the cytosolic and nuclear fractions indicating translocation of this fragment from the cytosol to the nucleus. Cell treatment with MG132 (0.1 µM, 4 h) strongly stabilized the ephrin-B2 ICD is efficiently degraded by the proteasome.

Fig.4: Treatment with EphB1 receptor increases phosphorylation of Src and FAK. A, B) ESdM were treated with EphB1 receptor and pSrc (Y418) detected by Western immunoblotting. Quantification shows increased levels of pSrc after 5-20 min of treatment (n=2). **C)** In-Cell Western analysis of EphB1 receptor treatment timeline vs Ctrl Fc treatment shows that EphB1 causes a significant increase of pSrc after 5 and 10 min in ESdM (n=3). **D)** ESdM were treated 10 min with Ctrl Fc or EphB1 receptor upon pre-treatment with a control solvent or DAPT. DAPT inhibits the EphB1-induced phosphorylation of Src. **E)** Quantification of D) (n=3). **F, G)** In-Cell Western analysis of Src and pSrc in primary microglia. Stimulation with soluble EphB1 increased pSrc. Inhibition of γ-secretase with DAPT prevented the increase in pSrc upon cell treatment with EphB1. **G)** Quantification of F) shows that treatment with EphB1 receptor for 10 min significantly increases pSrc levels. This stimulation is abrogated by the inhibition of γ-secretase with DAPT (n=3). **H)** EphB1 stimulation of ESdM cells causes a significant increase of pFAK levels after 5 minutes (n=3). **I)** Cells were treated 5 min with Ctrl Fc or EphB1 receptor. Pre-treatment with DAPT inhibits

EphB1-induced FAK phosphorylation. **J)** Quantification of I) (n=3). All data are represented as means ±SD.

Fig.5: Increased podosomal surface after γ-secretase inhibition and EphB1 stimulation. A) Schematic view of ESdM, showing leading and trailing edge and direction of migration. Red dots represent podosomes; box around the leading edge indicates image section displayed in B). **B)** Total internal reflection fluorescence (TIRF) microscopy of cells treated with either Ctrl Fc (DMSO Ctrl Fc) or EphB1 receptor (DMSO EphB1) in the absence or presence of DAPT and EphB1 receptor (DAPT EphB1). ESdM were stained with phalloidin (red) and a phosphotyrosine (pTyr) antibody (green). Scale bar: 20 μm. **C)** Quantification shows significantly increased levels of pTyr in the leading edge of EphB1 treated cells compared to Ctrl Fc treated cells. **D)** Quantification shows significantly increased actin levels in DMSO EphB1 and DAPT EphB1cells compared to DMSO Ctrl Fc cells. **E)** Quantification of the ratio between pTyr and actin shows no difference, demonstrating that protein phosphorylation correlates to podosomal surface. **F)** Comparison of delineated leading edge sizes shows no difference between the cell types. Each group contains a minimum of 35 cells. Data were collected in two independent experiments. All data are represented as means ±SD.

Fig.6: Impairment of γ-secretase increases the podosomal surface. A) PS1 full-length (FL) and C-terminal fragments (CTF) were detected by Western immunoblotting of isolated membranes from PSdKO cells re-expressing PS1 WT or PS1 DN (image for PS1 FL resulted from a longer exposure time than that for PS1 CTF). **B-D)** Quantification of pTyr and actin signals in the leading edge of cells imaged by TIRF microscopy. As compared to PSdKO cells re-expressing PS1 WT, PS1 DN expressing cells had significantly increased signals for pTyr and actin in the leading edge under unstimulated conditions. Stimulation with EphB1 increased signals for pTyr (B) and actin (C) in PS1 WT, but not in PS1 DN expressing cells. The ratio between pTyr and actin was similar under all conditions (D). Each group contains a minimum of 35 cells. Data were obtained from two independent experiments. All data are represented as means ±SD. **E)** Quantification of the leading edge surface showed no significant differences under all conditions.

Fig.7: Rescue of impaired phosphorylation of Src and FAK in cells without γ-secretase activity by re-expression of the ephrin-B2 ICD. A-D) Comparison of pSrc (A, B) and pFAK (C, D) levels in PSdKO cells transduced with either PS1 WT, PS1 DN or PS1

DN+ephrin-B2 ICD. Quantification revealed significantly reduced levels of pSrc (B) and pFAK (C) in PSdKO+PS1 DN cells, which can be rescued by additional stable transduction with ephrin-B2 ICD (n=6). All data are represented as means ±SD.

Fig.8: Functional involvement of the ephrin-B2 ICD in podosome structure. A) Total internal reflection fluorescence (TIRF) microscopy of PSdKO cells transduced with wild type PS1 (WT), dominant negative PS1 (DN) and PS1 DN cells expressing the soluble B2 ICD (PS1 DN+B2 ICD). ESdM were stained with phalloidin (red) and a phosphotyrosine (pTyr) antibody (green). Scale bar: 10 μm. **B-E)** Quantification of pTyr (B) and actin (C) showed significantly increased pTyr and actin signals in the leading edge of cells with inactive PS 1 (PS1 DN) as compared to cells with functional PS1 WT. Re-expression of the ephrin-B2 ICD in PS1 DN cells normalized pTyr and actin signals to that of PS1 WT expressing cells. The ratio of pTyr and actin was similar in all cell variants (D). The comparison of delineated leading edge sizes (E) shows increased size of the leading edge of PS1 DN as compared to PS1 WT cells. Re-expression of ephrin-B2 ICD in PS1 DN cells normalized the size if the leading edge to that of PS1 WT cells. Each group contains a minimum of 74 cells. Data were collected from two independent experiments. All data are represented as means ±SD.

Fig.9: γ-Secretase dependent regulation of microglial migration. A) Representative plots of random ESdM migration during 8 h time lapse microscopy after stimulation with CX3CL1 (15 ng/ml). CX3CL1 did not affect the proteolytic processing of epnrin B2 under these experimental conditions (not shown). **B)** Quantification revealed a significant reduction of the accumulated distance migrated by PSdKO+PS1 DN ESdM (PS1 DN) as compared to PSdKO+PS1 WT (PS1 WT) cells. Re-expression of the ephrin-B2 ICD in PSdKO+PS1 DN cells normalized migration. Each group contains a minimum of 44 cells. Data were obtained from three independent experiments. Manual tracking was done using ImageJ (Manual tracking plug-in). Plots as well as statistical data were obtained using the Ibidi chemotaxis and migration tool. **C)** Naïve ESdM cells (WT) or PSdKO cells re-expressing active PS1 WT (PS 1WT) or inactive PS 1 DN (PS1 DN) were treated with soluble EphB1 receptor in the absence or presence of DAPT. DMSO and Ctrl Fc alone served as treatment controls for DAPT and Eph B1Fc, respectively. Migration was analyzed as described in A, B. Migration of PS1 DN cells was significantly lower as compared to PS1 WT cells and naïve ESdM. Addition of EphB1 had no significant effect under these experimental conditions. The inhibition of γ-secretase with DAPT decreased the migration cells with functional γ-secretase

(naïve ESdM and PSdKO+PS1 WT). Each group contains a minimum of 18 cells. Data were collected from two independent experiments. All data are represented as means ±SD.

Fig.10: Schematic view of γ-secretase dependent regulation of microglial migration. Upon binding of the EphB1 receptor to the extracellular domain (A), ephrin-B2 undergoes ectodomain shedding by ADAM's (B). The resulting C-terminal fragment (CTF) is subsequently cleaved by γ-secretase within its transmembrane domain (C) thereby liberating the ephrin-B2 intracellular domain (ICD). The ICD can promote phosphorylation of Src and FAK possibly through binding to Src (D). The kinase activation of Src and FAK might regulate podosomal turn-over (E) and microglial migration (F).